Journal of Catalysis **188,** 215–225 (1999)
Article ID jcat.1999.2645, available online at http://www.idealibrary.com on IDEAL®

Catalytic Hydrogenation of Nitriles over Supported Mono- and Bimetallic Catalysts

Yinyan Huang and Wolfgang M. H. Sachtler

V. N. Ipatieff Laboratory, Center for Catalysis and Surface Science, Northwestern University, Evanston, Illinois 60201

Received May 21, 1999; revised July 30, 1999; accepted July 30, 1999

The bimetallic catalyst systems Pd–Ag/SiO_2, Pt–Sn/SiO_2, *M*–Cu/NaY (*M* = Ru, Rh, Pd, Pt), and *M*–Ni/NaY (*M* = Ru, Rh, Pd, Pt) have been tested for the gas phase hydrogenation of acetonitrile and butyronitrile in a fixed-bed microreactor and for the liquid phase hydrogenation of butyronitrile in an autoclave. Addition of *M* (*M* = Ru, Rh, Pd, Pt) to Ni promotes the reduction of Ni^{2+} and significantly increases the hydrogenation rate of butyronitrile in both the gas and the liquid phase. This enhanced activity is indicative of the formation of mixed ensembles on the surface of the bimetallic clusters. Addition of Sn to Pt decreases the activity for acetonitrile hydrogenation and improves the selectivity toward secondary amines. Addition of *M* (*M* = Ru, Rh, Pd, Pt) to Cu enhances the reduction of Cu^{2+} and lowers the activity for acetonitrile hydrogenation. Addition of Ag to Pd lowers the activity for acetonitrile hydrogenation. All *M*–Cu/NaY catalysts display high selectivity toward the formation of the secondary amine. The interaction between Ru and Ni depends on the Ru precursor; it is stronger with $RuCl_3$ than with $Ru(NH_3)_6^{3+}$. Addition of ammonia to the reaction mixture lowers the reaction rate, but increases the formation of primary amine.

I. INTRODUCTION

Bimetallic catalysts have been a favorite subject of fundamental research on heterogeneous catalysis and surface science for 7 decades. Spectacular deviations of catalytic activity and selectivity from the linear combination of the corresponding parameters for the monometallic counterparts have been found and models have been proposed to explain these effects. In the period 1930–1965 most authors assumed that the surface of an alloy had the same composition as the bulk, and long-range "collective" electronic effects, such as filling of the holes in the *d* band of a transition metal, were believed to be at the root of catalytic activity. In the 1960s evidence was published that even alloys such as Cu/Ni were biphasic when at equilibrium at the temperature used in numerous catalytic processes (1); moreover, it became clear that even for monophasic alloys the composition of the surface often deviates from that of the interior (2), and it depends strongly on the environment (3). Mere changes in collective electronic parameters have little effect on catalysis, but short-range effects and site geometry were found to be crucial (4). Surface science revealed that many adsorbates on a transition metal made use of "hollow sites"; for instance, at a close-packed crystal surface, three metal surface atoms are in direct contact with an adsorbed atom. For a binary alloy AB_x, the composition of such a triatomic adsorption site can be A_3, A_2B, AB_2, or B_3 with distinctly different heats of adsorption. In 1973 Sachtler coined the terms *ensemble effect* and *ligand effect* to facilitate the scientific discussion of these phenomena (5). Both effects contribute to the characteristic surface science when alloy surfaces interact chemically with their environment. We refer here only to review papers on well-defined alloys (6, 7), Somorjai's book (8), and an important paper by Rodriguez and Goodman (9).

For supported bimetal catalysts additional complications exist as different particles will have different compositions. Some metal precursors are incompletely reduced when present in isolation, but the presence of a second more noble metal often affects that reducibility (10, 11). Much attention has been focused on systems of a transition metal with high catalytic activity in hydrocarbon reactions (Pt, Ru, Pd, Rh, Ni,) and a second metal of low catalytic activity (Ag, Cu, Au, Sn). In this category it is meaningful to distinguish systems for which alloy formation is exothermic, such as Pt/Sn, and those for which it is endothermic, such as Pt/Au. A system that shows complete miscibility because alloy formation is neither exothermic nor endothermic is Pd–Ag; it is active for NO reduction by H_2 (12), diene hydrogenation (13–16), ethanol dehydrogenation (17), and selective conversion of chlorinated alkanes to alkenes (18). With exothermic alloys, intermetallic compounds of discrete composition are formed; a widely studied catalyst system in this category is Pt/Sn which is used in hydrocarbon reforming (19–22). Bimetallic systems for which alloy formation is endothermic include Ru–Cu, Pd–Cu, Rh–Cu, Pt–Cu, and Ni–Cu; among these Ru–Cu (23–27), Pt–Cu (28–31), and Pd–Cu (32–35) have been studied extensively as catalysts for hydrocarbon conversions or CO hydrogenation. Rh–Cu is active for benzene hydrogenation (36). Examples of much studied bimetallic catalysts in which both

0021-9517/99 $30.00

elements have high catalytic activity include Ru–Ni, which is active for the methanation of CO_2 with H_2 (23), and Rh–Ni, which catalyzes the partial oxidation of methane with O_2 (37, 38). The alloys Pd–Ni (11, 39) and Pt–Ni (40–43) are active hydrogenation catalysts.

The present research uses the hydrogenation of two nitriles, acetonitrile and butyronitrile, as probe reactions to investigate the effect of alloying on catalyst reducibility, activity, and selectivity. It is known that hydrogenation of a nitrile over a transition metal catalyst results in a variety of products: primary, secondary, and tertiary amines, unsaturated molecules such as enamines, and Schiff bases have been identified (44–47). In recent research the present authors found that all three amines are primary products, i.e., formed during a single residence at the metal surface (48, 49). Under conditions where the primary amine prevails over a ruthenium catalyst, secondary and tertiary amines abound over other transition metals, indicating that the nature of the metal surface is crucial for this selectivity. Preliminary results on the reaction mechanism should be faced with data on the effects of alloying on catalyst selectivity. Among the monometallic systems, Ru has the highest selectivity to primary amines. For hydrocarbon reactions the general experience is that alloying a metal such as Ru with high selectivity for hydrogenolysis and a "catalytically inert" metal, such as Ag, Au, or Sn, usually results in an enhanced ratio of catalytic hydrogenation to hydrogenolysis. It might therefore be expected that also for nitrile hydrogenation such dilution will alter the selectivity to primary vs secondary amines, as only the latter require fission of a C–N bond. There is, however, no evidence backing this simple speculation. Some patents exist mentioning bimetallic catalysts for nitrile hydrogenation. Rylander and Koch (50) used Ru–Pt, Ru–Pd, and Ru–Rh for the hydrogenation of aliphatic and aromatic nitriles, Borninkhof *et al.* (51) disclose the hydrogenation of alky nitriles over Ni–Cu chromite and Co–Cu chromite catalysts, and Vedage and Armor (52, 53) describe a process for the hydrogenation of butyronitrile to butylamine and dibutylamine over Al_2O_3-supported Ni–Ru, Ni–Rh, Ni–Cu, and Ni–Pd and Co–Rh, Co–Pd, and Co–Ni. In the scientific literature, Kumbhar *et al.* (54) report on the hydrogenation of benzonitrile over Ni–Cu and Kusaka *et al.* (55) on the hydrogenation of various nitriles over Ru–Co. These published data neither support nor negate the mechanistic speculation mentioned above.

In the present work, the bimetallic systems Pd–Ag, Pt–Sn, *M*–Cu (M = Ru, Rh, Pd, Pt), and *M*–Ni (M = Ru, Rh, Pd, Pt) have been studied for the hydrogenation in the gas or liquid phase of the two nitriles mentioned. Interest in this stage is focused on the enhanced reducibility of some systems and on catalyst *selectivity*, whereas the effects of alloying on the reaction rate will be presented mainly as changes of conversion at a given temperature. To minimize the effects of alloying on particle size, most tests were carried out with zeolite-supported metals or alloys, assuming that changes in particle size during reaction are small at the fairly low temperature used for the majority of these tests.

II. EXPERIMENTAL

II-1. Catalysts Preparation

1. Zeolite-supported monometallic catalysts. *M*/NaY (M = Ru, Ni, Rh, Pd, Pt, Cu) catalysts were prepared by ion exchange, as described previously (39, 56–60). NaY (UOP, Y-54) was used as received. Ru/NaY was prepared two different ways. Ru/NaY_a was prepared by ion exchange of $RuCl_3 \cdot xH_2O$ with Na/NaY at room temperature for 24 h. Ru/NaY_b was prepared by ion exchange of a $Ru(NH_3)_6Cl_3$ with NaY at room temperature (RT) for 24 h. Ni/NaY was prepared by ion exchange of $Ni(NO_3)_2$ with NaY at RT at a pH of ~6 for 24 h followed by a NaOH treatment; immediately after this exchange, the pH of the zeolite/water slurry was adjusted to a pH of ~10.0 by adding 0.5 M NaOH over 1 h with stirring. Stirring was continued for 1 h more, followed by filtering, washing with DDI H_2O, and drying in air. Rh/NaY was prepared by ion exchange of $Rh(NH_3)_5Cl_3$ with NaY at 80°C for 72 h. Pd/NaY was prepared by ion exchange of $Pd(NH_3)_4(NO_3)_2$ with NaY at RT for 24 h. Pt/NaY was prepared by ion exchange of $Pt(NH_3)_4(NO_3)_2$ with NaY at 80°C for 12 h. Likewise, Cu/NaY was prepared by slurrying $Cu(NO_3)_2$ and NaY at RT for 24 h. All *M*/NaY catalysts have a metal loading of about 3%.

2. NaY-supported bimetallic catalysts. All NaY-supported bimetallic catalysts were prepared by either simultaneous or successive ion exchange. Ru–Cu/NaY was prepared by a simultaneous ion exchange of $RuCl_3$ and $Cu(NO_3)_2$ with NaY at RT for 24 h. Pd–Cu/NaY was prepared by a simultaneous ion exchange of $Pd(NH_3)_4^{2+}$ and Cu^{2+} with NaY at RT for 24 h. Rh–Cu/NaY was prepared by ion exchanges of NaY with $Rh(NH_3)_5Cl^{2+}$ at 80°C for 12 h followed by secondary exchange with Cu^{2+} at RT for 24 h. Pt–Cu/NaY was prepared by ion exchange of NaY with $Pt(NH_3)_4^{2+}$ at 80°C for 12 h followed by secondary exchange with Cu^{2+} at RT for 24 h.

Ru–Ni/NaY samples were prepared by two methods: With Ru–Ni/NaY_a two-step ion exchange was used. Ni/NaY was precalcined in a flow of O_2 of 100 ml/min at 300°C for 2 h at a ramping rate of 0.5°C/min, redispersed in water, and exchanged with $RuCl_3$ at RT for 24 h. With Ru–Ni/NaY_b simultaneous ion exchange was applied by slurrying an aqueous solution of $Ru(NH_3)_6^{3+}$ and Ni^{2+} ions with NaY at RT for 24 h. This was followed by NaOH treatment as with the preparation of Ni/NaY. A two-step method was used for the preparation of Rh–Ni/NaY; ion exchange of NaY with $Rh(NH_3)_5Cl_3$ at 80°C for 12 h was followed by secondary ion exchange with $Ni(NO_3)_2$ at RT for 24 h and

subsequent treatment with NaOH as with Ni/NaY. Pd–Ni/NaY was prepared by ion exchange of precalcined Ni/NaY with $Pd(NH_3)_4^{2+}$ at RT for 36 h. A similar procedure was used for Pt–Ni/NaY; i.e., precalcined Ni/NaY was redispersed in water and exchanged with $Pt(NH_3)_4^{2+}$ ions at 80°C for 12 h.

All catalysts contain about 3% of Cu, Ru, Rh, Pd, and Pt. The actual metal loadings were determined by ICP analysis.

3. Silica-supported Pd–Ag and Pt–Sn catalysts. Pd–Ag/SiO_2 samples with 9% Pd loading and an Ag/Pd atomic ratio of 0.1, 1.0, and 2.0 were taken from those previously prepared by Sheu using conventional impregnation.

Pt–Sn/SiO_2 catalysts were prepared by co-impregnation of $Pt(NH_3)_4Cl_2$ and $SnCl_2 \cdot 2H_2O$ on silica. The catalysts have about 3 wt% Pt loading and the Sn/Pt ratios were 0.33, 1.0, and 2.0, respectively.

II-2. Catalysts Pretreatment and Reduction

After ion exchange, the Cu/NaY and *M*–Cu/NaY catalysts were calcined at 300°C to prevent migration of the Cu^{2+} ions into smaller zeolite cages (61). For Ru-containing catalysts calcination was carried out in He at 60 ml/min to prevent loss of the volatile Ru oxides; all other catalysts were calcined in an O_2 flow of 100 ml/min, increasing the temperature to 300°C at 0.5°C/min and holding at that temperature for 2 h.

Ni/NaY, Rh/NaY, Pd/NaY, Pt/NaY, RhNi/NaY, PdNi/NaY, and PtNi/NaY were calcined in an O_2 flow of 100 ml/min at 500°C for 2 h. The ramping rate was 0.5°C/min. Ru/NaY_a and $Ru–Ni/NaY_a$ were treated in a flow of Ar of 60 ml/min, while the temperature was increased to 450°C in 2 h and held there for 20 min.

$Ru–Ni/NaY_b$ was pretreated in three different ways. The first followed the procedure for $Ru–Ni/NaY_a$, i.e., calcination in a flow of Ar of 60 ml/min at 450°C for 20 min. The second procedure started with calcination of $Ru–Ni/NaY_b$ in a flow of Ar of 60 ml/min at 450°C for 20 min. This was followed by exposure to air at RT for 24 h and a second *in situ* calcination in a flow of Ar of 60 ml/min, while the temperature was increased to 500°C at a ramping rate of 0.5°C/min and held at 500°C for 2 h. The third followed the procedure for Ni/NaY, i.e., calcination in O_2 flow at 500°C.

Pt–Sn/SiO_2 catalysts were calcined in flowing oxygen of 100 ml/min at 450°C for 2 h with a ramping rate of 5°C/min.

The pretreated catalysts were subjected to TPR or reduction. Before gas phase reaction, all catalysts were reduced *in situ* in a H_2 flow of 30 ml/min. *M*–Cu/NaY catalysts were reduced at 500°C for 30 min with a ramping rate of 2°C/min. *M*–Ni/NaY catalysts were reduced at 500°C for 10 h with a ramping rate of 2°C/min. Pt–Sn/SiO_2 catalysts were reduced at 450°C for 8 h. Pd–Ag/SiO_2 samples were directly subjected to reduction at 450°C for 8 h. For liquid phase reaction, the catalysts are reduced *ex situ* under the same conditions and sealed in glass tubing under an Ar atmosphere.

II-3. TPR

Temperature-programmed reduction (TPR) was carried out in a flow of a 5% H_2/Ar mixture at 30 ml/min at 8°C/min. A thermal conductivity detector (TCD) monitored the H_2 consumption.

II-4. Catalytic Testing

Gas phase reaction was carried out in a microflow fixed-bed reactor, as described in our previous papers (60). The H_2 flow rate was 30 ml/min and the H_2/CH_3CN (or H_2/C_3H_7CN) molar ratio was 39. Usually, 100 mg of catalysts was used. Quartz (Fluka, <200 mesh) was used as the diluent when less than 100 mg of catalysts was used.

Liquid phase hydrogenation was carried out in a 300-ml autoclave (Autoclave Engineers, Inc.); 600 mg of catalyst was used for single-metal *M*/NaY catalysts and 300 mg for bimetallic *M*–Ni/NaY catalysts. The reaction mixture contained 0.05 mol of butyronitrile (4.3 ml) and 100 ml of heptane solvent. Before reaction, the glass tubing was cut and the prereduced catalyst was rapidly put into the reaction mixture. The system was purged with hydrogen for 15 min under stirring (300 rpm). Subsequently, H_2 at 24 bar was admitted into the autoclave at a stirring rate of 1500 rpm and the autoclave was heated to the reaction temperature (110°C). For the tests with ammonia, the reaction vessel was cooled in a dry-ice bath while catalysts and reactants were loaded and about 1.7 ml of liquid ammonia was added. The temperature inside the cell was about −57°C. After the autoclave was purged with hydrogen for about 15 min under stirring and the H_2 pressure was brought to about 24 bar in the closed autoclave, the dry-ice bath was removed. During heating and after the autoclave was heated to the reaction temperature (110°C), the total pressure was recorded. Samples of the reaction mixture were taken through the sampling valve at certain intervals and analyzed by GC. The reaction was stopped when the total pressure no longer changed.

III. RESULTS

III-1. TPR

1. M–Cu/NaY catalysts. TPR analysis of Ru–Cu/NaY, Rh–Cu/NaY, Pd–Cu/NaY, and Pt–Cu/NaY shows that addition of Ru, Rh, Pd, or Pt promotes the reduction of Cu^{2+}. In Fig. 1 the TPR profiles of Cu/NaY, Pt/NaY, and Pt–Cu/NaY are shown. The profiles of the other systems are similar. Cu/NaY has a TPR peak at about 300°C reduction and continues to 550°C. A weak negative peak at 629°C is probably due to reoxidation of Cu to Cu^+ by protons (62). Ru/NaY, Rh/NaY, Pd/NaY, and Pt/NaY display TPR peaks at 105, 93, 153, and 150°C, respectively. Addition of a second metal to Cu/NaY greatly enhances the reducibility of Cu^{2+}. For Ru–Cu/NaY, the reduction peak of Cu^{2+} shifts downward to

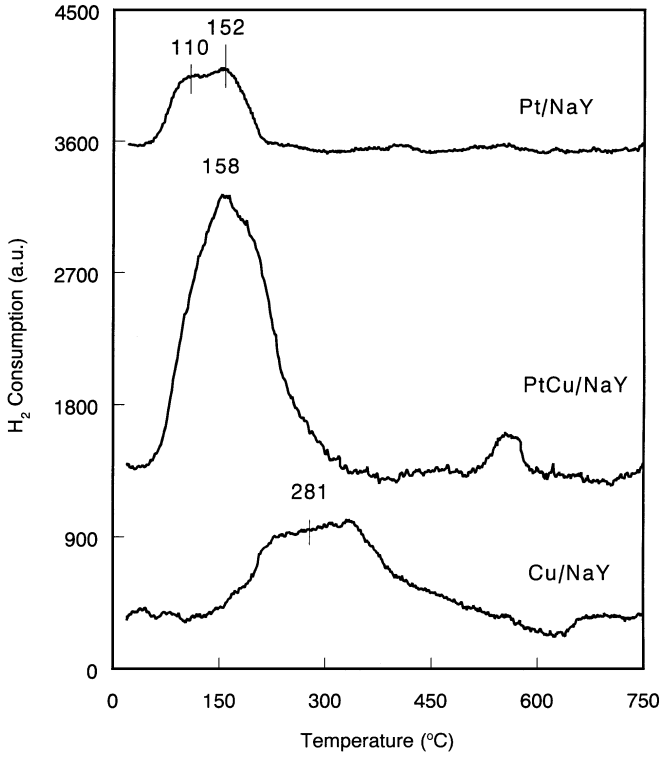

FIG. 1. TPR profiles of Cu/NaY, Pt/NaY, and Pt–Cu/NaY after calcination in O_2 at 300°C.

277°C, while for Rh–Cu/NaY, Pd–Cu/NaY, and Pt–Cu/NaY the reduction of Cu^{2+} is merged with the reduction of the noble metal ion and the TPR peaks are below 170°C.

2. Ru–Ni/NaY$_a$,M–Ni/NaY(M = Rh,Pd,Pt). TPR analysis also indicates that addition of Ru, Rh, Pd, and Pt promotes the reduction of Ni^{2+}, in agreement with the literature (39, 41). Figure 2 shows the TPR profiles of Ni/NaY, Pt/NaY, and PtNi/NaY. TPR profiles of other systems show similar features.

Ni/NaY calcined O_2 has a TPR peak at 474°C; reduction ceases at about 600°C. The peak corresponds to a H/Ni ratio of 1.6. It is very similar to the result found by Feeley *et al.* that about 86% of the Ni^{2+} can be reduced if Ni/NaY, prepared and treated under the same conditions, is reduced below 600°C (63). A small portion of Ni^{2+} requires a higher reduction temperature.

Ru/NaY$_a$ has a single reduction peak at 129°C. For Ru–Ni/NaY$_a$ three partially overlapping TPR peaks at 166, 201, and 304°C are observed. The peaks at 201 and 304°C are much weaker than the peak at 166°C. In comparison to Ru/NaY$_a$, the reduction of Ru^{3+} in Ru–Ni/NaY$_a$ is shifted to higher temperature; in contrast, the reduction of Ni^{2+} is shifted to lower temperature. Remarkably, the Ni^{2+} ions are completely reduced below 500°C; i.e., the presence of Ru in the sample greatly enhances the reduction of Ni^{2+}.

Rh/NaY has two unresolved TPR peaks at 91 and 187°C and a small peak at 632°C. The pattern is consistent with that published earlier (64). In the bimetallic system Rh–Ni/NaY, the TPR peak at 91°C can still be seen while the second peak is merged with the reduction peak of Ni^{2+}. Reduction of Ni^{2+} is clearly facilitated in the bimetallic system. The TPR peak at 470°C shifts to the much lower temperature of 353°C. However, a small portion of the Ni^{2+} remains difficult to reduce, as attested by the weak reduction peak of Rh at 632°C. Rhodium addition thus lowers the reduction temperature of the reducible fraction of the Ni in this zeolite without significantly lowering the fraction of the Ni that remains unreduced at 600°C.

Pd/NaY has a TPR peak at 167°C and a weak broad TPR peak at 579°C. For Pd–Ni/NaY, the TPR peak of Pd remains at 167°C but the reduction temperature for Ni^{2+} was lowered to 345°C. At the same time, a small portion of the Ni^{2+} ions in the bimetallic system is not reduced below 600°C.

Pt/NaY has two positive TPR peaks at 95 and 300°C and a negative TPR peak at 442°C. Integration of the two positive peaks leads to a H/Pt ratio of 2.72. That this value is larger than 2 indicates the presence of some PtO_2 besides PtO after calcination in O_2. The negative peak is attributed to reoxidation of Pt by protons that were formed during reduction at low temperature. This phenomenon was observed previously in this lab (65). For Pt–Ni/NaY, the reduction peak for Ni^{2+} merges with the peak of Pt^{2+} while some Ni^{2+} remains unreduced below 600°C.

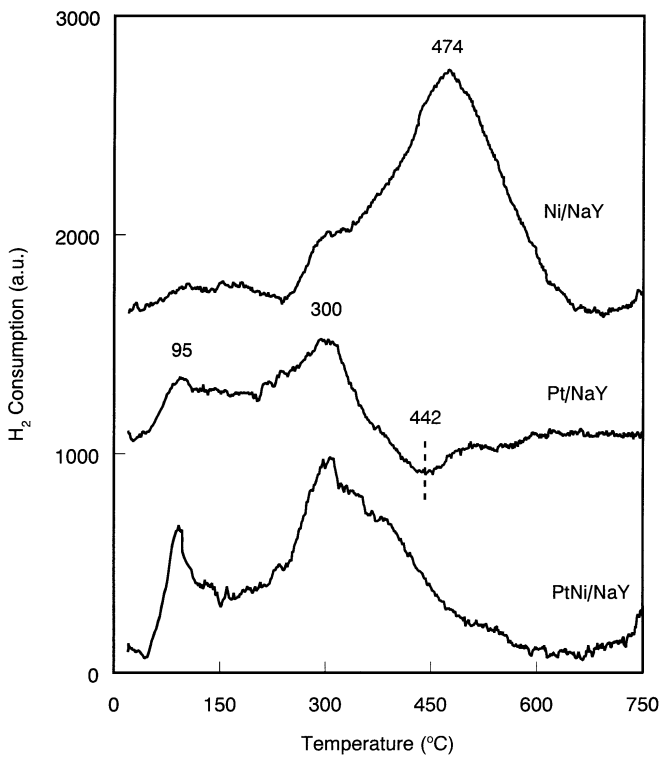

FIG. 2. TPR profiles of Ni/NaY, Pt/NaY, and Pt–Ni/NaY after calcination in O_2 at 500°C.

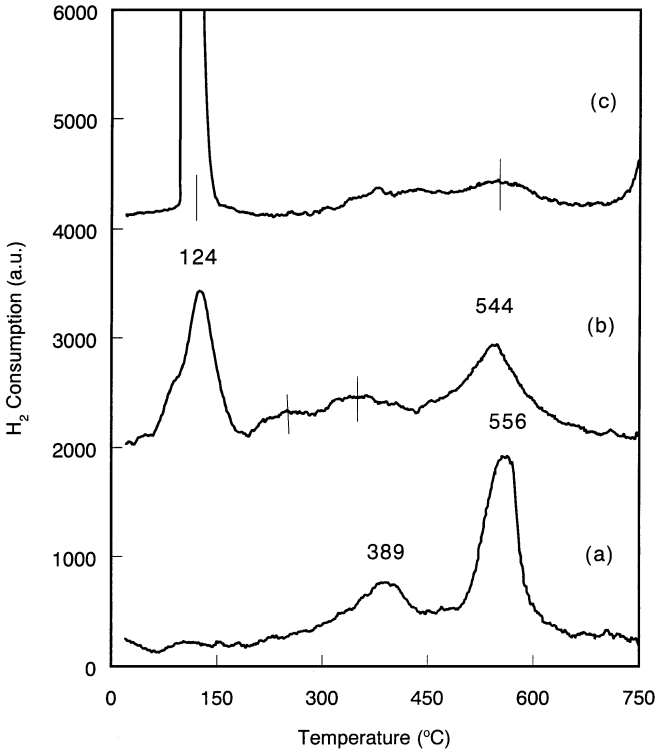

FIG. 3. TPR profiles of Ru–Ni/NaY$_a$ (a) after calcination in Ar at 450°C, (b) after calcination in Ar at 450°C, air at RT, and Ar at 450°C, and (c) after calcination in O_2 at 500°C.

3. Ru–Ni/NaY$_b$. The situation of Ru–Ni/NaY$_b$ is discussed separately due to its complexity. Various pretreatment conditions have been tried to promote the reducibility of nickel by Ru. The TPR profiles of Ru–Ni/NaY$_a$ prepared from $Ru(NH_3)_6Cl_3$ and treated under a variety of conditions are shown in Fig. 3.

No TPR peak is observed for Ru/NaY calcined in He. This sample looks gray and becomes black after contact with air at RT. However, if it is calcined again in He and reduced in H_2, the color returns to gray.

If Ru–Ni/NaY$_b$ is first calcined *in situ* in Ar, TPR analysis shows no reduction peak of Ru and two reduction peaks of Ni^{2+} at 389 and at 557°C. The peak at 557°C is much stronger than that at 389°C. Also, no TPR peak is observed above 600°C. Compared with that of Ni/NaY, it is clear that in the bimetallic system the reducibility of Ni^{2+} is increased below 600°C and some of the Ni is reduced more easily, but the majority of Ni^{2+} is reduced less easily.

If Ru–Ni/NaY$_b$ is first heated in Ar, then exposed to air for 24 h at RT, and re-heated in Ar at 500°C, the reduction of Ni^{2+} is found to be enhanced; i.e., the TPR peak for Ni^{2+} shifts to lower temperature and the peak at 554°C becomes smaller.

Upon treatment of Ru–Ni/NaY$_b$ in O_2 under the same conditions as those used for Ni/NaY, the reducibility of Ni^{2+} increases. The peak at about 540°C is weaker than that in Ni/NaY. A small portion of the Ni remains unreduced below 600°C. As for the large narrow peak that appears at 112°C, its size exceeds the response limit of the TCD detector. A rough estimate suggests that its hydrogen consumption is larger than H/Ru = 2 based on the Ru content of the fresh sample. Unfortunately, calcination of Ru catalysts in O_2 leads to the formation of highly volatile oxide RuO_4. It leads to a loss of Ru. Ru–Ni/NaY has an Ru/Al ratio of 0.418 after being heated in He, but has a ratio of 0.016 after calcination in O_2 at 400°C. Evidently, the majority of Ru is lost upon calcination in O_2. Based on the Ru content of the calcined Ru–Ni/NaY sample, the H/Ru value of the TPR peak at 112°C is much, much higher than 2, indicating condensation of RuO_4 in the exit area of the reactor and its reduction during TPR.

The above results indicate limited reduction enhancement when $Ru(NH_3)_6^{3+}$ was used as the precursor for the preparation of the Ru–Ni/NaY catalyst.

III-2. Catalytic Activity and Selectivity

1. Gas phase hydrogenation over SiO_2-supported bimetallic catalysts. Pd–Ag/SiO_2 catalysts were tested for gas phase hydrogenation of acetonitrile at 100°C. Ag/SiO_2 is totally inactive for this reaction. All active bimetallic catalysts deactivate during reaction to reach a steady state in which the activity decreases with the Ag/Pd ratio. For the Pd/Ag ratios 0, 0.1, 1, and 2, the specific steady state conversions of acetonitrile are (mol%) 26.0, 20.0, 19.0, and 11.3, respectively. A plot of the selectivities against the Ag/Pd ratio is shown in Fig. 4. Clearly, all catalysts of this group

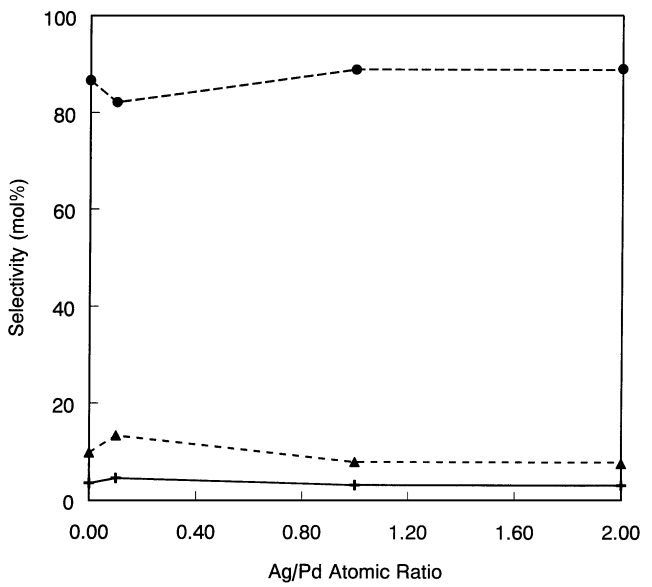

FIG. 4. Selectivity of gas phase hydrogenation of acetonitrile over Pd–Ag/SiO_2 at 100°C. (100 mg of catalysts, H_2 = 30 ml/min, H_2/nitrile = 39. ✚, ethylamine; ▲, diethylamine; ●, triethylamine.)

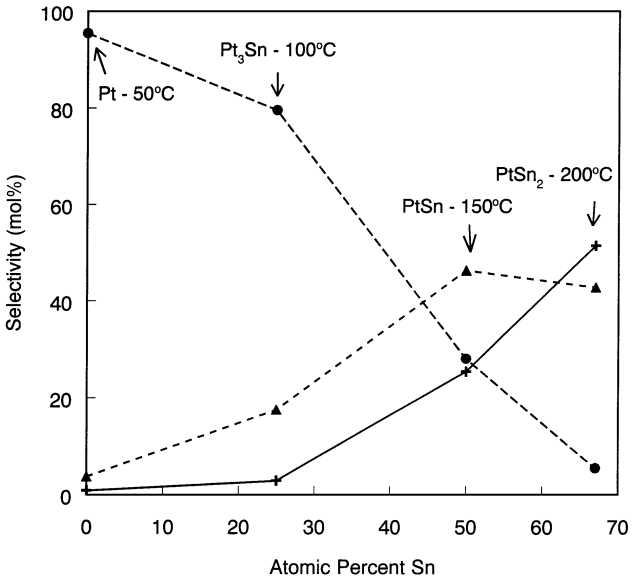

FIG. 5. Selectivity of gas phase hydrogenation of acetonitrile over Pt–Sn/SiO_2. (100 mg of catalysts, $H_2 = 30$ ml/min, H_2/nitrile = 39. Legends are the same as those in Fig. 4.)

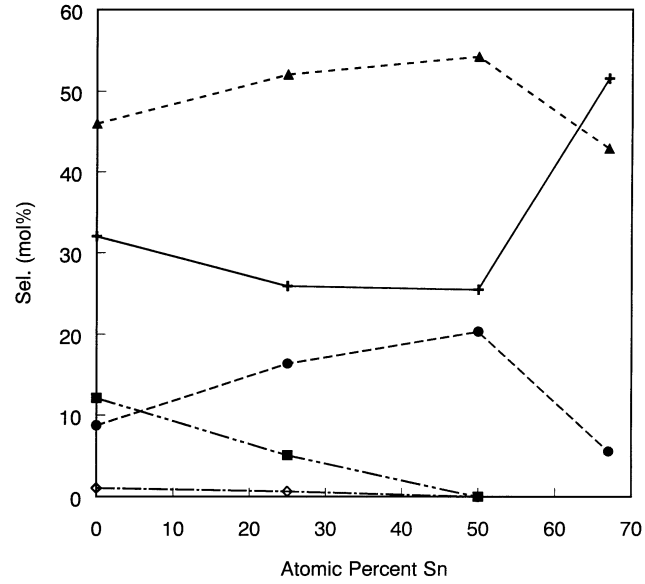

FIG. 6. Selectivity of gas phase hydrogenation of acetonitrile over Pt–Sn/SiO_2 at 200°C ($H_2 = 30$ ml/min, H_2/nitrile = 39. ■, ethylidene–ethylamine; ◇, ethane. Other legends are the same as those in Fig. 4.)

are highly selective to tertiary amine. The presence of Ag has no significant effect on the selectivity.

Pt–Sn/SiO_2 catalysts with about 3 wt% Pt loading were tested for the same hydrogenation. The Sn/Pt ratios were chosen to match those of the well-known intermetallic compounds in the Sn–Pt phase diagram. As expected, the addition of Sn to Pt greatly lowers the activity. To obtain a reasonable activity with Pt–Sn/SiO_2 catalysts, the reaction temperature had to be increased. All active catalysts deactivate with time; a steady state is reached at about 5 h time on stream. Figure 5 shows the selectivities of Pt–Sn/SiO_2 of different compositions at comparable conversions, i.e., at different temperatures. Whereas Pt/SiO_2 is highly selective to tertiary amine, this selectivity decreases upon increasing the Sn/Pt ratio and the temperature; concomitantly, the selectivity to primary amine increases.

To separate these variables and to demonstrate the effect of Sn addition on the selectivity, all catalysts were also tested at 200°C. For those with low Sn/Pt ratios, quartz was added as a dilutant to obtain conversions below 15%. The selectivities for acetonitrile hydrogenation at 200°C are shown in Fig. 6. The results show that Sn addition suppresses the hydrogenolysis of acetonitrile to ethane and ammonia. Pt–Sn catalysts of low Sn content further show the signature of Pt; i.e., the secondary amine is the preferred product except at very high Sn content where the primary amine prevails. However, even for the highest Sn content where conversion could be measured at this temperature, the selectivity toward ethylamine was only a little above 50%.

2. Gas phase hydrogenation of butyronitrile on bimetallic catalysts M–Cu/NaY. The bimetallic catalysts *M*–Cu/NaY (M = Ru, Rh, Pd, Pt) have been tested for gas phase hydrogenation and compared with monometallic catalysts. The catalysts deactivate with time. The reaction reaches steady state at 5 h time on stream. The results at steady state are summarized in Table 1. Whereas Cu/NaY is totally inactive for butyronitrile hydrogenation below 125°C, addition of Cu to monometallic catalysts significantly lowers their activity. The specific reaction rates (moles of nitrile converted $\times 10^{-3}$ per mole of metal per second) for the monometallic catalysts Ru, Rh, Pd, and Pt are 1.2, 6.8, 2.3, and 1.2 and for the bimetallic catalysts they are 0.44, 1.1, 0.23, and 0.31, respectively. Some bimetallic catalysts are all but

TABLE 1

Gas Phase Hydrogenation of Butyronitrile over Bimetallic *M*–Cu/NaY

Catalyst	T_{rxn} (°C)	Conv. (mol%)	Selectivity (mol%)			
			BA	BBA	DBA	TBA
Cu/NaY	125	0	—	—	—	—
Ru/NaY_a	115	6.7	44.2	40.9	13.7	1.1
Rh/NaY	110	36.6	13.5	1.9	68.1	16.4
Pd/NaY	125	12.3	5.0	0.3	63.5	31.1
Pt/NaY	125	34.5	1.7	0.4	35.5	62.4
Ru–Cu/NaY	115	2.4	3.6	1.0	72.6	22.7
Rh–Cu/NaY	110	6.0	12.0	2.1	75.9	10.0
Pd–Cu/NaY	125	1.2	5.2	0	83.8	11.0
Pt–Cu/NaY	125	0.9	5.8	0	80.6	13.6

Note. 100 mg of Catalyst, 30 ml/min of H_2, H_2/nitrile = 39, gas line heated; data at 5 h TOS; (BA) butylamine, (BBA) butylidene–Butylamine, (DBA) dibutylamine, (TBA) tributylamine.

TABLE 2

Gas Phase Hydrogenation of Butyronitrile over Bimetallic *M*–Ni/NaY

Catalyst	Conv. (%)	Sp act ($\times 10^{-3}$ s^{-1})	Selectivity (wt%) BA	BBA	DBA	TBA
Ni/NaY	23.4	2.47	19.9	9.9	37.9	32.3
Rh/NaY	11.7	2.67	45.2	12.0	40.4	2.5
Pd/NaY	1.0	1.81	2.6	0	88.1	9.3
Pt/NaY	8.6	2.81	0.8	0.6	23.1	75.5
Ru/NaY$_a$	0	0	—	—	—	—
Rh–Ni/NaY	91.1	6.58	34.2	0.3	44.2	21.2
Pd–Ni/NaY	97.9	7.09	49.7	0.1	39.6	10.6
Pt–Ni/NaY	91.0	7.16	44.0	0.6	41.6	13.8
Ru–Ni/NaY$_a$	46.8	2.98	41.6	7.4	28.2	22.8

Note. 100 mg of Catalyst, $H_2 = 30$ ml/min, H_2/nitrile = 39, 80°C, gas line heated; conv.-experimental conversion; data at 5 h TOS.

totally inactive. Whereas the monometallic catalysts of this group display high selectivity to either secondary or tertiary amine, the bimetallic catalysts show highest selectivity to secondary amine.

3. Bimetallic M–Ni/NaY catalysts for gas phase hydrogenation of butyronitrile. The single-metal catalysts Ni/NaY, Ru/NaY, Rh/NaY, Pd/NaY, and Pt/NaY as well as the bimetallic catalysts *M*–Ni/NaY were tested for gas phase hydrogenation at low temperature, i.e., for the single-metal catalyst in the kinetic regime. All catalysts deactivate with time until they approach a steady state at 5 h. Deactivation is more obvious for Ru–Ni/NaY(a) than for the others, probably due to residual chlorine in Ru–Ni/NaY(a). The steady state activity and selectivity data are compiled in Table 2. The specific activities of the bimetallic catalysts are much higher than those of the monometallic counterparts. Since all catalysts were reduced under the same conditions, their dispersions will be similar. Therefore, the present results indicate a rather dramatic synergistic effect between two metals. Over some bimetallics the conversion approaches 100%; i.e., the true rate constants could be orders of magnitude higher than those over the single-metal catalysts.

The results over Ru–Ni/NaY$_b$ are not included in Table 2 because the conversions over this catalyst depend on the pretreatment conditions. No synergetic effect is observed when the catalyst is pretreated in inert gas while pretreatment in O_2 leads to the loss of Ru due to the formation of volatile Ru oxides.

The selectivities of the bimetallic catalysts differ markedly from those of the single-metal catalysts. In general, Ru catalyzes preferentially the formation of primary amines, while Ni, Rh, and Pd favor the formation of secondary amines, and Pt is selective toward the formation of tertiary amines. These selectivities have been found in our work and in that of other authors (44). It is remarkable that the combination of Ni with Pd, i.e., two metals with high selectivity for the secondary amine, results in a catalyst with 50% selectivity to the primary amine. Also, the other bimetallic *M*–Ni catalysts show a higher selectivity than Ni/NaY to primary amine. The selectivity toward the primary amine of Rh–Ni/NaY is, however, lower than that of Rh/NaY. With $M =$ Pt, Rh, or Pd, the selectivity toward the unsaturated intermediate butylidine–butylamine (BBA) is extremely low. If this simply meant higher hydrogenation activity, one would expect an enhanced selectivity for the secondary amine, which is, however, contrary to the experimental facts.

4. Liquid phase hydrogenation of butyronitrile over monometallic and bimetallic catalyst. Liquid phase hydrogenation of butyronitrile has been carried out with Ru/NaY, Rh/NaY, Pd/NaY, Pt/NaY, Ni/NaY, Ru–Ni/NaY$_a$, Rh–Ni/NaY, Pd–Ni/NaY, and Pt–Ni/NaY at 110°C. Conversions and selectivities are summarized in Table 3. In most cases the run was stopped when conversion was 90% or higher; the reaction times have been specified in the table.

In general, the bimetallic catalysts achieve high conversion in significantly shorter times than the single-metal catalysts, with the exception of the very active Rh/NaY, although in these tests the amount of bimetallic catalysts was only half that of the monometallic catalysts. Clearly, the bimetallic catalysts are much more active than the monometallic catalysts. This result is consistent with that obtained with the gas phase reaction.

Significant differences in selectivity exist between the catalysts. Ru/NaY shows highest selectivity to the primary amine; Rh/NaY and Ni/NaY show highest selectivity to the secondary amine, but their selectivities to primary amine are still rather high; Pd/NaY and Pt/NaY produce almost exclusively the secondary amine.

The selectivities of all bimetallic catalysts differ from those of the corresponding monometallic catalysts.

TABLE 3

Liquid Phase Hydrogenation of Butyronitrile over *M*–Ni/NaY

Catalyst	Wt (mg)	t_{rxn} (h)	Conv (%)	Selectivity (mol%) BA	BBA	DBA	TBA
Ni/NaY	600	3	99.8	23.5	0.3	61.2	15.0
Ru/NaY$_b$	600	8	89.2	67.9	22.8	9.2	0.1
Rh/NaY	600	2	93.8	44.2	4.5	51.0	0.2
Pd/NaY	600	7	89.9	3.6	0.1	94.8	1.4
Pt/NaY	600	7	75.9	2.9	0.1	88.8	7.3
Ru–Ni/NaY$_a$	300	2.25	100	61.8	0.1	35.6	2.6
Rh–Ni/NaY	300	1.5	99.8	50.5	0.2	46.1	3.2
Pd–Ni/NaY	300	1.75	100	29.2	0	65.5	5.3
Pt–Ni/NaY	300	1.25	99.9	38.2	1.2	53.0	7.6

Note. 110°C, 0.05 mol of nitrile, 24 bar of H_2, 100 ml of heptane, 1500 rpm.

Formation of the unsaturated molecule BBA is very low over the bimetallic catalysts. Ru–Ni/NaY and Rh–Ni/NaY show the highest selectivity to primary amine while Pd–Ni/NaY and Pt–Ni/NaY preferentially form the secondary amine.

All catalysts show a low, but detectable, activity for hydrogenolysis of the CN bond to produce butane and ammonia. Butane has been detected with GC-MS. The highest butane selectivity of 0.8% is observed with Pt/NaY at 110°C. Due to the low boiling point of butane, it is actually possible that this molecule is somewhat underestimated by GC. Butane formation has also been detected in the gas phase hydrogenation of butyronitrile.

5. Liquid phase hydrogenation of butyronitrile in the presence of ammonia over M–Ni/NaY catalysts. Many authors hydrogenated nitriles in the presence of a considerable pressure of ammonia, to shift equilibria of the type $R_2NH + NH_3 = 2RNH_2$ toward the primary amines. Accordingly, the present authors have tested *M*–Ni/NaY catalysts (M = Ru, Rh, Pd, Pt) by carrying out liquid phase hydrogenation of butyronitrile in the presence of ammonia at 110°C. Table 4 shows the conversion and selectivity after a certain reaction time. Clearly, the presence of ammonia lowers the rate of nitrile hydrogenation. For example, with Ru–Ni/NaY only 2.25 h is needed to reach complete conversion in the absence of ammonia, but with ammonia only 87.1% conversion is reached after 8 h. As expected, the presence of ammonia enhances the yield of the primary amine. Over Ru–Ni/NaY the selectivity to the primary amine is 91.5% in the presence of ammonia, but only 61.8% in its absence at 100% conversion. The same effect was observed over Rh–Ni/NaY and Pt–Ni/NaY.

The situation over Pd–Ni/NaY is different. Initially, the concentration of primary amine in the reaction mixture is high, exceeding that obtained without ammonia. However, after about 4 h on stream (about 56% conversion), the concentration of the primary amine becomes lower than that of the secondary amine; the composition of the final reaction mixture is similar in the presence of ammonia and in its absence at similar conversion.

TABLE 4

Liquid Phase Hydrogenation of Butyronitrile over *M*–Ni/NaY Catalysts in the Presence of Ammonia

Catalyst	*t* (h)	Conv (%)	Selectivity (mol%) BA	BBA	DBA	TBA
Ru–Ni/NaY$_a$	8	87.1	91.5	2.8	5.7	0
Rh–Ni/NaY	5	79.1	81.2	3.4	7.6	0.2
Pd–Ni/NaY	5.5	72.8	29.0	0.7	68.2	2.1
Pt–Ni/NaY	3	88.5	70.7	1.4	27.2	0.6

Note. 110°C, 300 mg of catalyst, 0.05 mol of butyronitrile, 1.7 ml of liquid NH_3, 100 ml of heptane.

V. DISCUSSION

The present findings on reducibility enhancement are in line with general experience. The reduction of metal ions by H_2 to metal particles can be visualized as consisting of two main steps: nucleation and then growth. In bimetallic systems the noble metal will be reduced first; ions of the second metal can attach themselves to the clusters of the noble metal, where H_2 will be dissociatively adsorbed. Reduction and formation of a bimetallic cluster are completed when H^+ ions are released to the support. As a result, the reduction of the second metal takes place at significantly lower temperature than that in the absence of the noble metal. For instance, Ni^{2+} ions can join Pd_3 clusters:

$$Pd_3^0 + Ni^{2+} = [Pd_3Ni]^{2+},$$

$$[Pd_3Ni]^{2+} + H_2 \Rightarrow HPd_3NiH]^{2+} \Rightarrow [Pd_3Ni]^0 + 2H^+.$$

If amminated transitions metal ions, such as $Pd(NH_3)_4^{2+}$, are used in the ion exchange, this chemistry is complicated by autoreduction of these ions. Autoreduction of metal–ammine complexes in zeolites has been observed by Gallezot (66, 67) and ourselves for all heavy Group VIII metals and is quite a general phenomenon (68–70). The extent of autoreduction is known to depend on the rate of calcination of the catalyst precursor after ion exchange. A high flow rate of oxygen and low heating rate were shown by Gallezot to minimize autoreduction of Pd. With Pt it is impossible to suppress autoreduction. In the case of Pd, the Pd_n nuclei tend to agglomerate to larger Pd particles, and consequently, less alloy formation will take place. During calcination in oxygen, the autoreduced metal clusters will be transformed to oxide clusters. With Rh it has been shown that the oxide particles react with zeolite protons so that Rh^{3+} ions are regenerated (71).

The shift of the TPR profiles to lower temperature demonstrates that the reduction of Ni^{2+} is enhanced by the presence of Rh, Pd, and Pt, indicating alloy formation. Surprisingly, integration of the TPR profiles shows that the percentage of the Ni^{2+} which is reduced below 600°C remains roughly the same in monometallic and bimetallic *M*–Ni/NaY samples with M = Rh, Pd, Pt. However, it should be noted that these TPR runs were carried out in a 5% H_2/Ar mixture with a ramping rate of 8°C/min, whereas the *in situ* reduction of the catalysts prior to testing was carried out in a pure H_2 flow with a ramping rate of 1°C/min, followed by holding the temperature at 500°C for 10 h. After such extensive reduction treatment our data indicate that all Ni is reduced to Ni^0 in the bimetallic catalysts.

With Ru–Ni, alloy formation in zeolite cages is more complicated. TPR results indicate that ruthenium has a smaller effect than other transition metals on the enhancement of the reducibility of nickel when $Ru(NH_3)_6^{3+}$ is used as the precursor. A number of possible causes can be visualized:

(1) Treatment with NaOH immediately after ion exchange will cause agglomeration of Ni^{2+} ions to form $Ni(OH)_2$ gel, while $Ru(NH_3)_6^{3+}$ ions do not agglomerate but remain dispersed in the supercages. This scenario favors phase separation: Ru^0 and small NiO particles are formed after heating in Ar or He. No strong reducibility enhancement of Ni^{2+} or alloy formation is expected, if contact between Ru^0 and NiO is limited. This phase separation model is supported by observations with Pd–Ni/NaY for which TPR after calcination in He or Ar shows no reduction peak of Pd^{2+}. Thus, although autoreduction of Pd^{2+} by NH_3 is known to take place, the Pd^0 has no significant effect on the reduction of Ni^{2+}. The TPR profile of Pd–Ni/NaY looks very similar to that of Ni/NaY. Calcination at higher temperature leads only to a shift of the reduction peak for Ni^{2+} to higher temperature. This TPR profile is totally different from that after calcination in O_2. It seems that, for Pd–Ni/NaY, calcination in He leads to segregation of Pd particles and limited alloy formation. In contrast, calcination in O_2 leads to the formation of PdO and NiO, which strongly interact with each other. Therefore, the reducibility of Ni is greatly enhanced after this treatment.

(2) Ru^0 clusters in NaY cages that are obtained by ion exchange of $Ru(NH_3)_6^{3+}$, followed either by autoreduction or by controlled reduction with H_2, have been reported to be very sensitive to O_2 to form RuO_2 (56, 72–74). This neutral oxide will easily agglomerate and move out of the zeolite upon heating. Separation of RuO_2 and NiO particles in Ru–Ni/NaY inhibits reducibility enhancement of Ni^{2+}.

(3) Agglomeration of RuO_2 and formation of volatile RuO_4 take place when Ru–Ni/NaY is calcined in O_2. This volatilization is documented for Ru supported on NaY or SiO_2 (72, 75). Accordingly, the Ru loading of Ru/SiO_2 decreases by calcination in O_2 at 260°C from 1% to 0.62% (76). Loss of Ru also leads to a visible change in color from black to grey for Ru/NaY heated in O_2 at 400°C. At the same time, some dark material, presumably condensed RuO_4, is deposited at the reactor walls and the frit. This material is very difficult to dissolve in aqua regia; no such deposit was, however, observed when Ru–Ni/NaY is calcined in O_2. In this case the color of the material remains darker than the grey monometallic Ru/NaY. Element analysis showed that the Ru/Al ratio of Ru/NaY is 0.417 after heating in He, but 0.002 after calcination in O_2 at 400°C. In contrast, the Ru/Al ratio of Ru–Ni/NaY is 0.418 after heating in He, but 0.016 after calcination in O_2 at 400°C. The presence of Ni^{2+} apparently helps to retain some Ru. The effects of Ru on reducibility and catalysis in these samples are thus caused by a very small amount of Ru. Possibly, a small quantity of a Ru–Ni alloy is present in the reduced bimetallic catalysts.

Whereas the above data suggest a rather weak effect of Ru on the reducibility of Ni, a significant enhancement of Ni reduction by Ru is observed if $RuCl_3$ is used as the precursor of Ru. Also, a more active catalyst is obtained with this precursor containing significant amounts of Ru–Ni alloy clusters. Even simple impregnation of $RuCl_3$ with Ni/NaY results in a good Ru–Ni/NaY catalyst. An alternative procedure will be ion exchange of Ru^{3+} with Ni/NaY, as described for the preparation of Ru–Cu/NaY. In the absence of NH_3, no autoreduction takes place; upon calcination in an inert gas (He, Ar) the Ru^{3+} ions lose their H_2O ligands and become well dispersed on the inner surface of the zeolite or attached to the surface of NiO clusters. After co-reduction of Ni and Ru, Ru–Ni alloy clusters are formed.

For *M*–Cu/NaY bimetallic systems, the present TPR results demonstrate that the reduction of Cu^{2+} is enhanced by the presence of Ru, Rh, Pd, and Pt, indicating, again, strong interaction between two metals and alloy formation. The chemistry sketched here has been used to optimize alloy formation in zeolite-supported multimetal catalysts for the hydrogenation of nitriles. In view of the enhanced activity of *M*–Ni/NaY catalysts in butyronitrile hydrogenation this could be of practical value.

Turning now to activity and selectivity, it is obvious from the present results that the conversion over alloyed Ni catalysts is much higher than over monometallic Ni; the enhancement exceeds the amount predicted on the basis of additivity or enhanced reducibility of the nickel. It is also evident from the present results that alloying has a profound effect on the selectivity. Formation of the unsaturated molecule BBA is very low over the bimetallic catalysts, indicating the relative favorization of saturation of the double bond. The selectivity to primary amine is high over Ru–Ni/NaY and Rh–Ni/NaY, though lower than that over Ru/NaY, whereas Pd–Ni/NaY and Pt–Ni/NaY preferentially form the secondary amine.

In the Introduction the concept of atomic ensembles in the surface of an alloy was mentioned. As pointed out there and in other papers (6, 77–82), a decreasing ensemble size of atoms of the most active metal will lead to suppressed hydrogenolysis and enhanced hydrogenation selectivity. Obviously, the simple idea that selectivity might be controlled by the hydrogenolytic splitting required for the formation of higher amines is not helpful to rationalize the present results. No correlation of hydrogenolysis activity and formation of higher amines is found. Diluting Pd ensembles by an inactive metal such as Ag or Sn addition to Pt, though suppressing the hydrogenolysis of acetonitrile to ethane, does not strongly change the catalytic signature of Pt to secondary amines. Only at very high Sn content does the expected formation of primary amine become evident, but this selectivity does not much exceed 50%.

The heat of chemisorption on mixed ensembles will be between the values for the pure ensembles of the same size of either metal. In terms of the Balandin theory a volcano-shaped curve relates the catalytic activity with the heat of

adsorption. A strongly enhanced activity is predicted for bimetallic catalysts, if the values for the pure metals are located at different sides of the volcano. This is apparently the case for the present systems for which strong enhancement of the catalytic activity has been found in the present work.

The position of the maximum depends, of course, on the nature of the reactant. For the hydrogenation of benzonitrile over the silica-supported Ni catalysts. Kumbhar *et al.* (54) found that the catalytic activity was lower when Ni was alloyed with copper. Likewise, the present results show that, for gas phase hydrogenation of acetonitrile, addition of Ag to Pd, or Sn to Pt and/or Cu to Ru, Rh, Pd, and Pt leads to decreased catalytic activity.

The results on the activity changes due to alloying can thus be rationalized in terms of mixed ensembles with intermediate heat of adsorption. The catalytic reaction rate will be higher than that of the most active alloy partner, if the heats of chemisorption on both pure metals are located at different sides of the volcano-shaped curve. Unfortunately, no predictive conclusions on activity and selectivity appear warranted at the present stage.

The present results further show not only that addition of ammonia to the reactant mixture shifts the equilibrium of the three amines toward the primary amine, as predicted by thermodynamics, but also that ammonia also interferes with the reaction mechanism. As a strong competitor for active sites, it lowers the reaction rate significantly.

CONCLUSIONS

(1) Addition of Ru, Rh, Pd, or Pt to Ni/NaY enhances the reduction rate of Ni and strongly increases the catalytic activity for the hydrogenation of butyronitrile. The enhanced activity is predominantly attributed to mixed ensembles in the surface of bimetal clusters.

(2) Addition of Ru, Rh, Pd, or Pt to Cu/NaY enhances the reduction rate of Cu^{2+} but lowers the activity for acetonitrile hydrogenation. All Cu–*M*/NaY catalysts show high selectivity to secondary amine.

(3) Addition of Sn to Pt lowers the activity of Pt for acetonitile hydrogenation and promotes the formation of secondary amine.

(4) Strong interaction between Ru and Ni is obtained if $RuCl_3$ is used as the precursor for the preparation of Ru–Ni/NaY.

(5) Ammonia lowers the reaction rate but improves the formation of primary amine.

ACKNOWLEDGMENTS

The authors thank the management of Air Products and Chemicals, Inc., for funding this research and kindly permitting publication of this report. We also thank Dr. J. N. Armor for many elucidating discussions.

REFERENCES

1. Sachtler, W. M. H., Dorgelo, G. J. H., and Jongepier, R., *J. Catal.* **4**, 100 (1965).
2. Sachtler, W. M. H., *J. Catal.* **4**, 654 (1965); Sachtler, W. M. H., and Jongepier, R., *J. Catal.* **4**, 665 (1965).
3. Bouwman, R., and Sachtler, W. M. H., *J. Catal.* **19**, 127 (1970).
4. Sachtler, W. M. H., and van der Plank, P., *Surf. Sci.* **18**, 62 (1969).
5. Sachtler, W. M. H., *Le Vide* **164**, 19 (1973).
6. Sachtler, W. M. H., and van Santen, R. A., *Adv. Catal.* **26**, 69 (1977).
7. Campbell, C. A., *Adv. Catal.* **36**, 1 (1989).
8. Somorjai, G. A., "Chemistry in two dimensions: Surfaces." Cornell University Press: Ithaca, NY/London, 1981.
9. Rodriguez, J. A., and Goodman, D. W., *Surf. Sci. Rep.* **14**, 108 (1991).
10. Augustine, S. M., Nacheff, M. S., Tsang, C. M., Butt, J. B., and Sachtler, W. M. H., *in* "Proceedings, 9th International Congress on Catalysis, Calgary, Canada, 1988" (M. J. Phillips and M. Ternan, Eds.) Vol. 3, p. 1190. Chem. Institute of Canada, Ottawa, 1988.
11. Feeley, J. S., and Sachtler, W. M. H., *Zeolites* **10**, 738 (1990).
12. Naito, S., and Tanaka, Y., *in* "Proceedings, 11th International Congress on Catalysis, Baltimore, 1996" (J. W. Hightower, W. N. Delgass, E. Iglesia, and A. T. Bell, Eds.), Part A&B, p. 1115. Elsevier, Amsterdam, 1996.
13. Sarkany, A., *Appl. Catal.* **165**, 87 (1997).
14. Sarkany, A., *Catal. Deact. 1997* **111**, 111 (1997).
15. Sales, E. A., Benhamida, B., Caizergues, V., Lagier, J. P., Fievet, F., and Bozon-Verduraz, F., *Appl. Catal. A* **172**, 273 (1998).
16. Venezia, A. M., Liotta, L. F., Deganello, G., Schay, Z., and Guczi, L., *J. Catal.* **182**, 449 (1999).
17. Cao, Y., Liu, B. S., and Deng, J. F., *Appl. Catal.* **154**, 129 (1997).
18. Heinrichs, B., Delhez, P., Schoebrechts, J. P., and Pirard, J. P., *Prep. Catal. VII* **118**, 707 (1998).
19. Verbeek, H., and Sachtler, W. M. H., *J. Catal.* **32**, 257 (1976).
20. Coq, B., and Figueras, F., *J. Mol. Catal.* **25**, 87 (1984).
21. Palazov, A., Bonev, C., Shopov, D., Lietz, G., Sárkány, A., and Völter, J., *J. Catal.* **103**, 249 (1987).
22. Lin, L. W., Zhang, T., Zang, J. L., and Xu, Z. S., *Appl. Catal.* **67**, 11 (1990).
23. Elliott, D. J., and Lunsford, J. H., *J. Catal.* **57**, 11 (1979).
24. Sinfelt, J. H., *J. Catal.* **29**, 308 (1973).
25. Sinfelt, J. H., Lam, Y. L., Cusumano, J. A., and Barnett, A. E., *J. Catal.* **42**, 227 (1976).
26. Schoenmaker-Stolk, M. C., Verwijs, J. W., and Scholten, J. J. F., *Appl. Catal.* **30**, 339 (1987).
27. Crisafulli, C., Maggiore, R., Scirè, S., Galvagno, S., and Milone, C., *J. Mol. Catal.* **83**, 237 (1993).
28. Bouwman, R., and Sachtler, W. M. H., *J. Catal.* **26**, 63 (1972).
29. Moretti, G., and Sachtler, W. M. H., *J. Catal.* **15**, 205 (1989).
30. Tzou, M. S., Kusunoki, M., Asakura, K., Kuroda, H., Moretti, G., and Sachtler, W. M. H., *J. Phys. Chem.* **95**, 5210 (1991).
31. Han, D. H., Lee, J. S., Nomura, M., Sachtler, W. M. H., Moretti, G., Woo, S. I., and Ryoo, R., *J. Catal.* **133**, 191 (1992).
32. Nosova, L. V., Zaikovskii, V. I., Kalinkin, A. V., Talzi, E. P., Paukshtis, E. A., and Ryndin, Yu. A., *Kinet. Catal.* **36**, 328 (1995).
33. Choi, K. I., and Vannice, M. A., *J. Catal.* **131**, 36 (1991).
34. Noronha, F. B., and Schmal, M., *Appl. Catal.* **78**, 125 (1991).
35. Fernández-García, M., Márquez Alvarez, C., and Haller, G. L., *J. Phys. Chem.* **99**, 12566 (1995).
36. Tebassi, L., Sayari, A., and Ghorbel, A., *J. Mol. Catal.* **25**, 397 (1984).
37. Yan, Q. G., Yu, Z. L., and Yuan, S. Y., *Chem. J. Chinese Univ.* **19**, 626 (1998).
38. Leu, F. C., and Chang, T. H., *J. Chinese Inst. Chem. Eng.* **30**, 81 (1999).
39. Feeley, J., and Sachtler, W. M. H., *J. Catal.* **131**, 573 (1991).
40. Massardier, J., and Bertolini, J. C., *J. Catal.* **90**, 358 (1984).

41. Jiang, H. J., Tzou, M. S., and Sachtler, W. M. H., *React. Kinet. Catal. Lett.* **35**, 207 (1987).
42. Bertolini, J. C., and Massardier, J., *Catal. Lett.* **9**, 183 (1991).
43. Raab, C. G., and Lercher, J. A., *Catal. Lett.* **18**, 99 (1993).
44. Volf, J., and Pašek, J., *in* "Catalytic Hydrogenation" (L. Červený, Ed.), p. 105. Elsevier, Amsterdam, 1986.
45. De Bellefon, C., and Fouilloux, P., *Catal. Rev. Sci. Eng.* **36**, 459 (1994).
46. Barrault, J., and Pouilloux, Y., *Catal. Today* **37**, 137 (1997).
47. Peterson, R. J., *Chem. Technol. Rev.* **94**, 229 (1977).
48. Huang, Y.-Y., and Sachtler, W. M. H., *Appl Catal A* **182**, 365 (1999).
49. Huang, Y.-Y., and Sachtler, W. M. H., *J. Catal.* **184**, 247 (1999).
50. Rylander, P. N., and Koch, J. H., Jr., U.S. Patent, 3,177,258 (1965).
51. Borninkhof, F., Kuijpers, E. G. M., and Berben, P. H., U.S. Patent, 5,235,108 (1993).
52. Vedage, G. A., and Armor, J. N., U.S. Patent, 5,567,847 (1996).
53. Vedage, G. A., and Armor, J. N., U.S. Patent, 5,574,189 (1996).
54. Kumbhar, P. S., Kharkar, M. R., Yadav, G. D., and Rajadhyaksha, R. A., *J. Chem. Soc., Chem. Commun.* 584 (1992).
55. Kusaka, H., Hara, Y., Onuki, M., Akai, T., and Okuda, M., *J. Catal.* **161**, 96 (1996).
56. McCarthy, T. J., Marques, C. M. P., Trevinõ, H., and Sachtler, W. M. H., *Catal. Lett.* **43**, 11 (1997).
57. Shoemaker, R., and Apple, T., *J. Phys. Chem.* **91**, 4024 (1987).
58. Treviño, H., and Sachtler, W. M. H., *Catal. Lett.* **27**, 251 (1994).
59. Jiang, H. J., Tzou, M. S., and Sachtler, W. M. H., *Catal. Lett.* **1**, 99 (1988).
60. Huang, Y. Y., and Sachtler, W. M. H., *J. Phys. Chem. B* **102**, 6558 (1998).
61. Ichikawa, T., and Kevan, L., *J. Phys. Chem.* **87**, 4433 (1983).
62. Lei, G. D., Adelman, B. J., Sárkány, J., and Sachtler, W. M. H., *Appl. Catal. B* **112**, 245 (1995).
63. Feeley, J., Ph.D. thesis, Northwestern University, Evanston, IL, 1992.
64. Tomczak, D. C., Lei, G. D., Schünemann, V., Treviño, H., and Sachtler, W. M. H., *Micropor. Mater.* **5**, 263 (1996).
65. Tzou, M. S., Teo, B. K., and Sachtler, W. M. H., *J. Catal.* **113**, 220 (1988).
66. Gallezot, P., Alarcon-Diaz, A., Dalmon, J. A., Renouprez, A. J., and Imelik, B., *J. Catal.* **39**, 334 (1975).
67. Gallezot, P., and Bergeret, G., *in* "Catalyst Deactivation" (Z. Peterson and A. T. Bell, Eds.), p. 287. Marcel Dekker, New York, 1987.
68. Homeyer, S. T., and Sachtler, W. M. H., *J. Catal.* **117**, 9 (1989).
69. Homeyer, S. T., and Sachtler, W. M. H., *J. Catal.* **118**, 266 (1989).
70. Carvill, B. T., Lerner, B. A., Zhang, Z. Z., and Sachtler, W. M. H., *J. Catal.* **143**, 314 (1993).
71. Tomczak, D. C., Zholobenko, V. L., Treviño, H., Lei, G. D., and Sachtler, W. M. H., *in* "Zeolites and Related Microporous Materials: State of the Art 1994" (J. Weitkamp, H. G. Karge, H. Pfeifer, and W. Hölderich, Eds.), Part B, p. 893. Elsevier, Amsterdam, 1994.
72. Zou, W., and Gonzalez, R. D., *J. Catal.* **133**, 202 (1992).
73. Pedersen, L. A., and Lunsford, J. H., *J. Catal.* **61**, 39 (1980).
74. Fiedorow, R. M. J., Chahar, B. S., and Wanke, S. E., *J. Catal.* **51**, 193 (1978).
75. Kobylinski, T. P., Taylor, B. W., and Young, J., *Trans. Soc. Auto. Eng.* **83**, 1089 (1974).
76. Lopez, T., Herrera, L., Gomez, R., Zou, W., Robinson, K., and Gonzalez, R. D., *J. Catal.* **136**, 621 (1992).
77. Ponec, V., *Catal. Rev. Sci. Eng.* **11**, 41 (1975).
78. Sachtler, W. M. H., *Catal. Rev. Sci. Eng.* **14**, 193 (1976).
79. Sinfelt, J. H., *Adv. Catal.* **23**, 91 (1976).
80. Ponec, V., *Adv. Catal.* **32**, 149 (1983).
81. Sachtler, W. M. H., *CHEMTECH* **7**, 434 (1983).
82. Biswas, J., Bickle, G. M., Gray, P. G., Do, D. D., and Barbier, J., *Catal. Rev. Sci. Eng.* **30**, 161 (1988).